Liquid Crystals
Publication details, including instructions for authors and subscription information:
http://www.informaworld.com/smpp/title~content=t713926090

The realignment of an achiral smectic C chevron structure with applied field

Alison Findon; Helen F. Gleeson; John E. Lydon

To cite this Article Findon, Alison , Gleeson, Helen F. and Lydon, John E.(2002) 'The realignment of an achiral smectic C chevron structure with applied field', Liquid Crystals, 29: 1, 79 — 85
To link to this Article: DOI: 10.1080/02678290110086497
URL: http://dx.doi.org/10.1080/02678290110086497

LIQUID CRYSTALS, 2002, VOL. 29, NO. 1, 79–85

The realignment of an achiral smectic C chevron structure with applied field

ALISON FINDON, HELEN F. GLEESON*
Department of Physics and Astronomy, Manchester University,
Manchester M13 9PL, UK

and JOHN E. LYDON
Department of Biochemistry, Leeds University, Leeds LS2 9JT, UK

(*Received 15 May 2001; accepted 2 July 2001*)

This is the second of two papers describing the study of a conventional display cell filled with an achiral smectic C phase. In our first paper we described the X-ray diffraction study of the smectic layer alignment in the cell in its initial 'off' state. The mesogen used has positive dielectric anisotropy and the cell surfaces were treated conventionally to give a parallel homogeneous alignment. The X-ray results were interpreted in terms of a complex three-component chevron pattern with two outer arms and a central, tilted bookshelf region. This paper concerns the change in optical texture of the cell as the applied field is increased. There is a sequence of reversible texture changes before the final irreversible breakdown of the structure. The optical data are consolidated by electro-optic and field-dependent X-ray data. We interpret the changes in optical texture in terms of a sequence of four distinct realignment processes as the field is increased: (1) re-alignment of the molecules within the existing layer structure by rotation of the director around the smectic C cones; (2) growth of the two outer chevron arms at the expense of the central bookshelf region; (3) a progressive modification of the domain structure; (4) an abrupt, drastic, irreversible re-alignment at high field with complete breakdown of the original chevron structure to a quasi-homeotropic structure.

1. Introduction

The study of layer geometries in smectic devices is a subject of considerable interest. The layer structure adopted within a device has a significant impact on its optical and electro-optical properties. It is well known that the layer shrinkage that occurs on cooling to a tilted chiral smectic C phase from a smectic A phase frequently induces a chevron structure [1]. Such chevron structures also occur in antiferroelectric, ferrielectric [2] and even smectic A devices [3]. The occurrence of a chevron structure has an impact not only on device properties in the context of commercial applications, but also on the interpretation of experimental data. This is particularly important where electric fields are applied such as in Fréedericksz transition experiments, when the initial layer geometry and field-induced chevron to bookshelf transitions can complicate the interpretation of transition thresholds.

In our previous publication, we described the study of a conventional display cell filled with an achiral smectic C (SmC) mesogen [4]. The device was originally intended to be used for the evaluation of layer elastic constants according to the Fréedericksz transition experiments suggested by Carlsson *et al.* [5]. Such experiments relied on a specific, uniform alignment of the layers within the device. From a study of the X-ray diffraction pattern of this device (or to be more precise, from a study of the way in which the X-ray diffraction pattern of the cell changed with rocking angle), we concluded that there was a three-component chevron structure in the field-off state, as sketched in figure 1. As one might expect, bearing in mind the difference between the two flexing elastic constants for a SmC layer (A_{12} and A_{21}), the layers appear to be curved significantly in one direction, and more or less flat in the other. In this paper, the way in which the optical texture changed with applied field, and the extent to which this texture change is reversible when the imposed field is removed, are described and discussed. It is important to understand the field-induced deformation of a complex chevron structure such as is adopted in this device to allow a better understanding of the elastic constants of smectic C systems and chevron structures as a whole.

---

*Author for correspondence;
e-mail: Helen.Gleeson@man.ac.uk

Liquid Crystals ISSN 0267-8292 print/ISSN 1366-5855 online © 2002 Taylor & Francis Ltd
http://www.tandf.co.uk/journals
DOI: 10.1080/02678290110086497

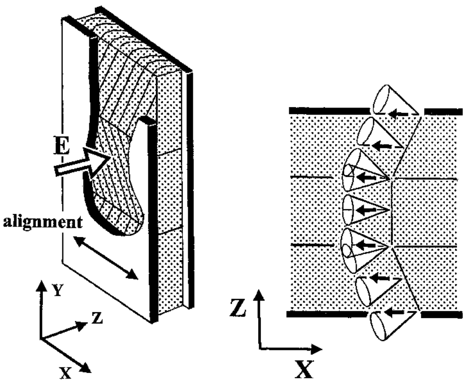

(*a*) (*b*)

Figure 1. The three-branched chevron structure postulated in our earlier paper [4] as the structure of the field-off state. This structure arises from the differential shrinking of the structure along the Y-direction at the N–SmC transition when the cell is filled. Note the distinction between this 3-component chevron structure and the familiar two-component chevron structure of chiral C* phases (where the suppression of the chiral twist results in the progressive rotation of the molecular director as one passes through the cell in the Z-direction). (*a*) Sketch of the cell showing the three-branched chevron in the XZ-plane and the tilted zigzag in the YZ-plane. Details of the arrangement of additional layers at the boundaries between the domains, to preserve the layer continuity, have been omitted. Also omitted in this sketch is the significant curvature of the layers in the XZ-plane, discussed in our earlier paper [4]. The double-headed arrow lying parallel to X indicates the surface alignment direction. (*b*) View of an XZ-section of the cell showing the orientation of the alignment cones for the three parts of the chevron structure for zero field.

2. Experimental detail

The full details of the materials used and experimental techniques employed are described in our previous publication [4]. Flat cells of nominal thickness 4 or 8 μm were prepared with parallel glass windows and contained homogeneously aligned samples of the room temperature smectogenic mixture, M3. This mixture [4] is achiral and has positive dielectric anisotropy, exhibiting smectic-C and nematic phases with transition temperatures $T_{\mathrm{SmCN}} = 45°\mathrm{C}$ and $T_{\mathrm{NI}} = 86°\mathrm{C}$. The cell windows were of 100 μm thick glass, making them thin enough for both optical and X-ray diffraction studies. The surfaces were coated with a conducting layer of indium tin oxide and treated with rubbed PVA to give a parallel, homogeneous alignment.

The optical textures were observed with an Olympus BH2 polarizing microscope fitted with a Linkam hot stage. Electro-optic traces were recorded with the sample held in the same hot stage on an optical rail between crossed polarizers. A laser diode provided the light source and the transmitted light was detected using a photodiode and amplifier with a linear intensity response. The X-ray diffraction experiments were carried out on station 2.1 at Daresbury Laboratory SRS, Warrington, UK. Temperature control was provided by a modified Linkam hot stage held in a goniometer arrangement that allowed rocking to specific angles of interest. Sinusoidal fields with a frequency of 1 kHz were applied to the device using a signal generator and wide band amplifier, identical apparatus being used for both the optical and X-ray measurements.

3. Results: description of the changes in optical texture with applied field

The sequence of optical micrographs in figure 2 shows the changes in appearance of a cell of thickness 3.8 μm when viewed between crossed polarizers as the amplitude of the imposed field is increased from zero to 24 V $\mu\mathrm{m}^{-1}$ (90 $\mathrm{V}_{\mathrm{rms}}$). There is a complex series of reversible texture changes before the irreversible realignment of the structure that occurs at high voltages (around 10 V $\mu\mathrm{m}^{-1}$, 40 $\mathrm{V}_{\mathrm{rms}}$) at the temperature selected for this device (38°C). Figure 3 shows the electro-optic response of the device, while figure 4 gives complementary X-ray data. Figure 4 (*a*) shows the rocking curve for the device, indicating peaks at rocking (device tilt) angles of 0° and around 17° consistent with the presence of both bookshelf and chevron regions in the sample. Figure 4 (*b*) shows the way in which the intensity of the X-ray Bragg diffraction peak, observed at a rocking angle of 17° (the chevron angle of the device), varies over the same range of applied field for a thicker device (8 μm). The symbols A–F in figure 3 indicate the conditions at which each micrograph in figure 2 was recorded. Details of the process of field-induced realignment are discussed in the context of the micrographs, and the electro-optic and the X-ray diffraction data shown in figure 3 and 4, respectively.

3.1. *Zero field*

The appearance of the texture for zero field is shown in figure 2(A). The cell, as seen between crossed polarizers, has an overall banded appearance with broad bands running more or less parallel to the (molecular) alignment at the surfaces. Within the bands there is some diagonal detail with a resemblance to the so-called herringbone texture sometimes observed in lyotropic hexagonal phases. Bearing in mind our earlier X-ray diffraction studies [4], we interpret these bands in terms of the domain pattern shown in figure 1.

3.2. *Low applied fields*

Study of the photomicrographs of figure 2 show that the overall director field, i.e. the pattern of division of the mesophase into domains, appears to be unchanged for fields up to ~10 V $\mu\mathrm{m}^{-1}$ (40 $\mathrm{V}_{\mathrm{rms}}$ for the 3.8 μm

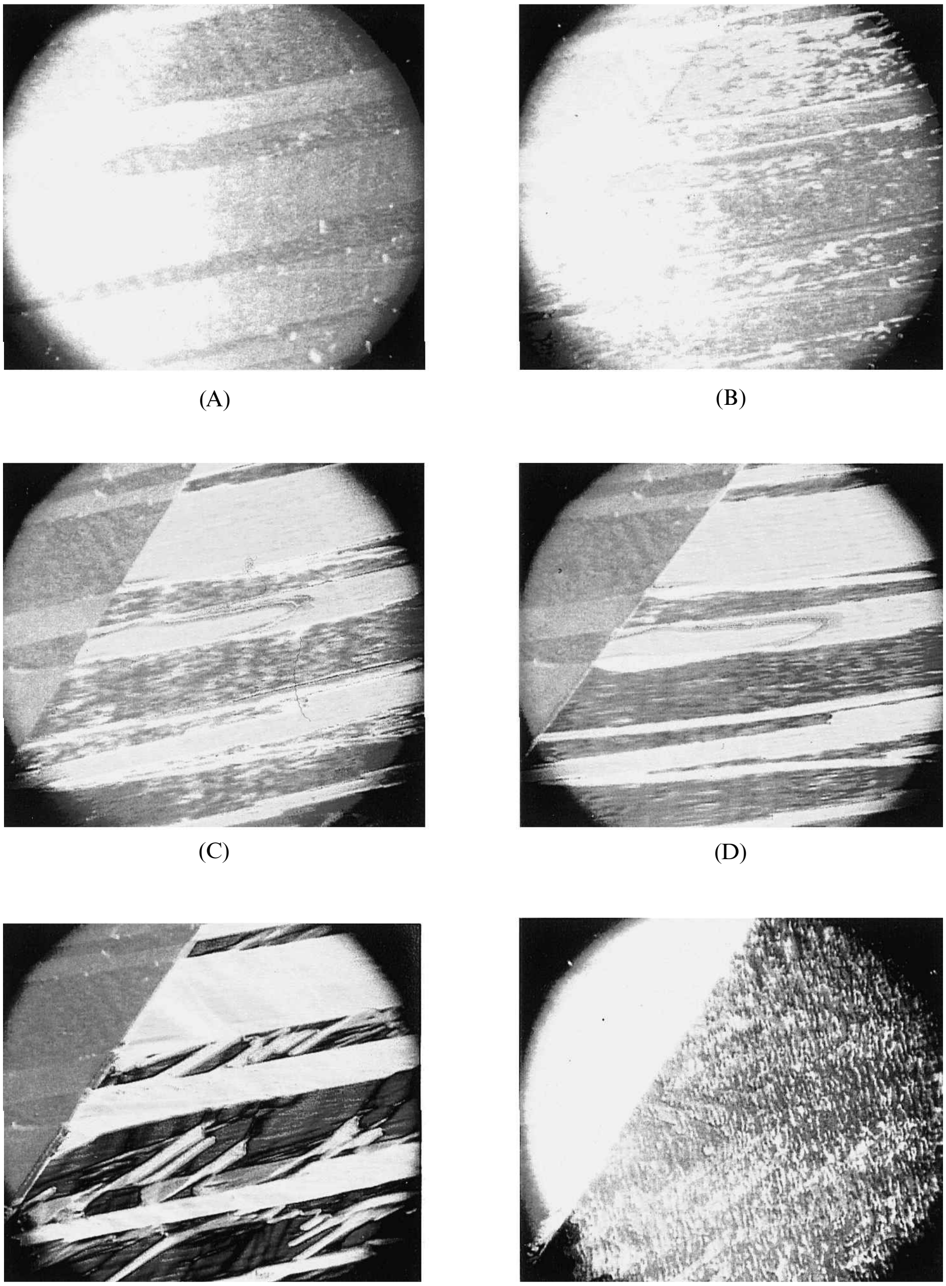

(A) (B)

(C) (D)

(E) (F)

Figure 2. Optical textures at different applied field strengths: (A) no field (B) 10.5 V_{rms} (C) 12.9 V_{rms} (D) 25.3 V_{rms} (E) 46.0 V_{rms} (F) 91.0 V_{rms}. The segment at the upper left hand side of each micrograph shows a region not covered by the electrodes. The cell thickness was 3.47 μm, the temperature was 38.4°C and the frequency 1 kHz. In all cases, the cells were viewed between crossed polarizers.

thick device studied in this experiment). However, the birefringence colours shown by the separate domains do not remain constant: the pale blue areas become darker and the greenish areas become bright yellow. Such information can be interpreted in the context of a change in effective birefringence of the sample. Although interpretation of colours is somewhat subjective, it appears that birefringence colours are becoming 'purer' indicating a shift to lower order interference colours with the molecular realignment—cf. figure 2(A) and 2(C). The textural observations agree well with the electro-optic data of figure 3. There is a large change in transmitted intensity at approximately 10 V_{rms} (2.7 V μm^{-1}), consistent with the observed change in birefringence colours

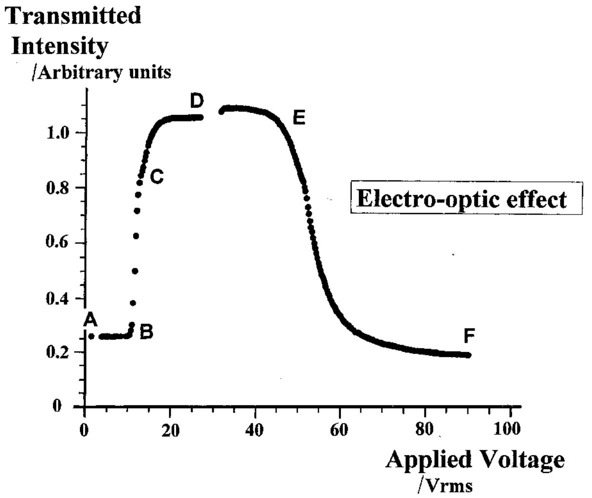

Figure 3. The electro-optic plot for M3 showing the variation of transmitted intensity with applied field strength (for the same device as used to obtain the optical micrographs shown in figure 2). The letters A–F indicate the transmittance levels for the voltages at which photographs shown in figure 2 were taken.

of the device. Following this initial change, there is little change in the transmitted intensity at low applied fields.

As the voltage is increased, a further effect is seen in the textures which is less apparent in the electro-optic data. There is a progressive readjustment of the domain boundaries with invasion of the dark blue regions by parallel sided strips of yellow domains inclined at range of angles. As is apparent in figures 2(C) and 2(D), asymmetric islands appear within some of the large domain regions. The islands are bounded by narrow lightning zigzags on one side and broad vertical bands on the other. Features of this type are familiar in defect states of chiral smectic C cells [1].

It is worth comparing the textural observations with the X-ray data of figure 4. Figure 4 (*a*) shows the rocking curve obtained for the device. Here, it can be seen from the relatively strong Bragg peaks around 0° and the chevron angle of 17° that the sample has both bookshelf and chevron structure. For the electric field experiment, the device was held at the rocking angle of 17° and the intensity of the Bragg peak monitored. Little change in the peak intensity is observed at low applied fields, indicating that there is no drastic layer reorganization in this regime.

3.3. *High voltages*

There is a relatively sudden change in texture when the applied field reaches approximately 10 V μm^{-1}. The domain structure present throughout the previous sequence is lost (except for the merest shadow) and a pattern of vertically-elongated linear domains is created.

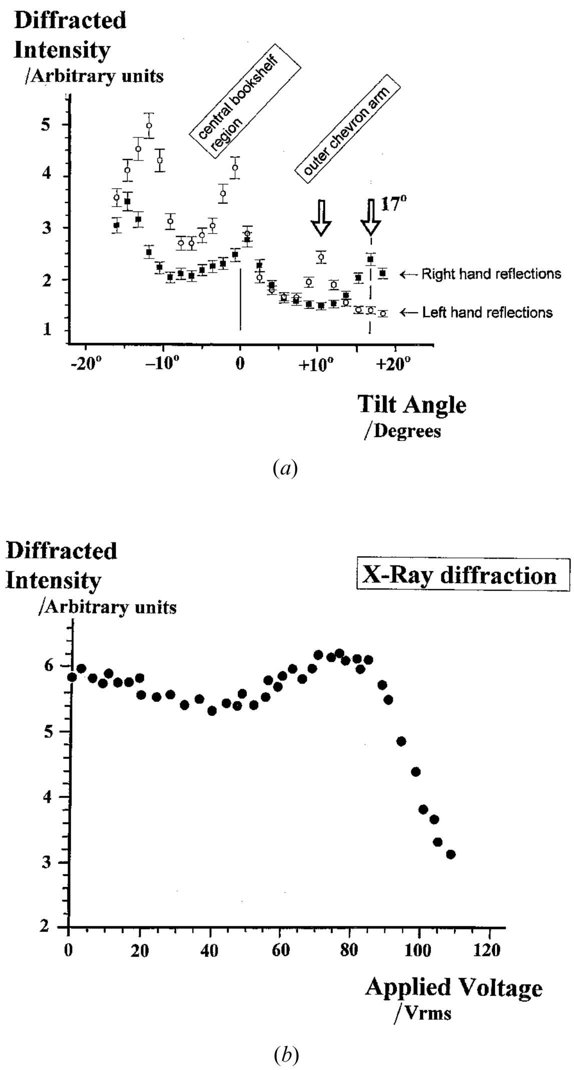

(*a*)

(*b*)

Figure 4. (*a*) The variation of diffracted intensity with rocking (device tilt) angle. Each of the three regions of the chevron pattern (i.e. the central bookshelf and the two outer arms) gives rise to two Bragg reflections recorded on the area detector used (corresponding to reflections from the 'front' and the 'back' of the planes). The open arrows at + 14° and + 17° indicate the two Bragg reflecting positions for one of the outer arms. (*b*) Change of diffracted X-ray intensity with applied voltage. This plot shows the variation of the integrated intensity against applied voltage for a sample of M3 in a cell thickness 8 μm at a temperature of 37°C. The sample was held at a rocking angle of 17° whilst the data were recorded. (This orientation corresponds to the Bragg reflecting position for one of the outer chevron arms.) The abrupt fall in scattered intensity at an applied voltage of ~90 V corresponds to the drastic high field realignment. Note that this occurs at a higher voltage than the high field transition apparent in the electro-optic plot shown in figure 3 because of the greater cell thickness.

The textural observations are confirmed by the electro-optic and field-dependent X-ray scattering intensity of figures 3 and 4(*b*). Both data sets show a gross and relatively sudden change at similar field strengths, indicating a significant movement of layers out of the Bragg condition at the rocking angle chosen and a concurrent change in effective birefringence of the sample.

3.3. *Reversibility*

The ability of the cell to recover its original texture when the applied field was switched off was investigated. Figure 5 shows the appearance of the 3.8 μm thick device shortly after fields of different amplitudes were removed. It is apparent that, for low applied fields, under approximately 3 V μm^{-1}, the texture change was completely reversible and the cell reverted to the initial texture. For higher voltages, the recovery was less complete and above the voltage of catastrophic realignment (approximately 90 V for a 3.8 μm cell) the original texture was completely lost.

4. Discussion: explanation of the texture changes

The electric field response of the smectic C material in the planar device is discussed in the context of the complex chevron structure previously postulated for this system [4] and its field-induced modification. We suggest that the first response is a realignment of the molecules within the existing layers, with the molecular directors pictured as rotating round the smectic C cones, figure 6(*a*). They rotate until they lie as close to the direction of the applied field as they are able, without disturbing the layer structure. For molecules with positive dielectric anisotropy and positive optical anisotropy this would involve a reduction in the perceived birefringence of each part of the sample as shown in figure 6(*b*), and hence explain the observed colour changes and electro-optic response. In this context, the sample is undergoing a Fréedericksz transition of the *c*-director at a field of approximately 2.7 V μm^{-1}. A more detailed examination of the transition thresholds and associated measurements of elastic constants with respect to device thickness and temperature is reported elsewhere [6].

There are two distinct types of domain in the low field SmC chevron structure: the outer arms and the central bookshelf region. During the second stage of the response, we suggest that there is growth of the outer arms at the expense of the central region. As shown in figures 7(*a*) and 7(*b*), the orientations of the alignment cones of the two outer arms allow the molecules there to align closer to the applied field direction than those of the central region. This must make the outer chevron regions more stable than the inner bookshelf part and we would expect therefore that the central bookshelf region would gradually disappear as the boundaries converge towards the centre of the device. We have no way of seeing this postulated effect directly using optical microscopy, but the suggestion is not incompatible with

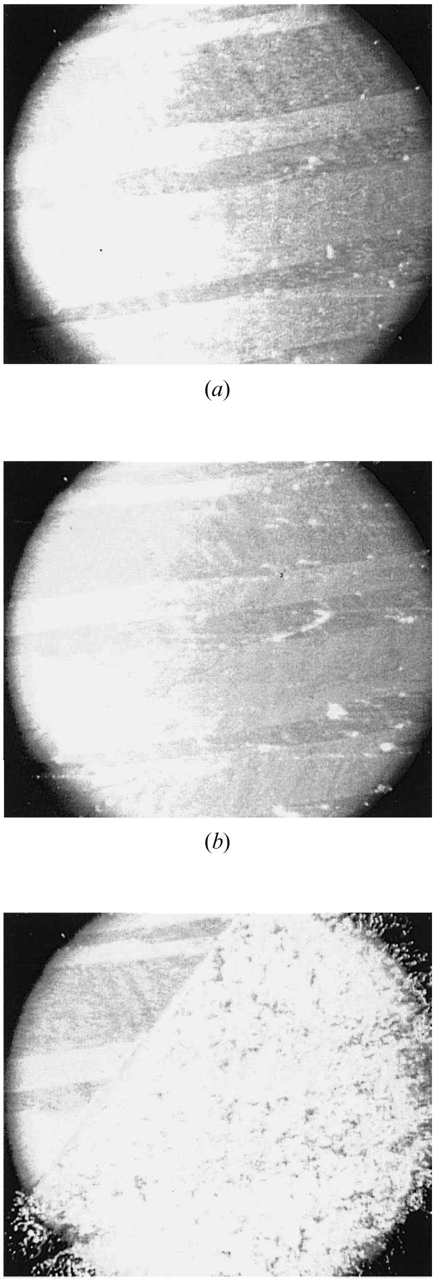
(*a*)

(*b*)

(*c*)

Figure 5. Retention of optical texture when the applied field was switched off. These optical micrographs show the appearance of the cell a few minutes after the field was removed. Figures 5(*a*), 5(*b*) and 5(*c*) refer to initial voltages of 10.5, 25.3 and 91.0 V_{rms} respectively and should be compared with figures 2(B) 2(D) and 2(F), respectively. It is apparent that for applied voltages $<12\ V_{rms}$ the texture change was completely reversible and the cell reverted to the initial state, whereas for higher voltages, the recovery was less complete. Above the voltage of catastrophic realignment (approximately 90 V for a 3.8 μm cell) the original texture was completely lost. The experimental details are the same as those given in the caption for figure 2.

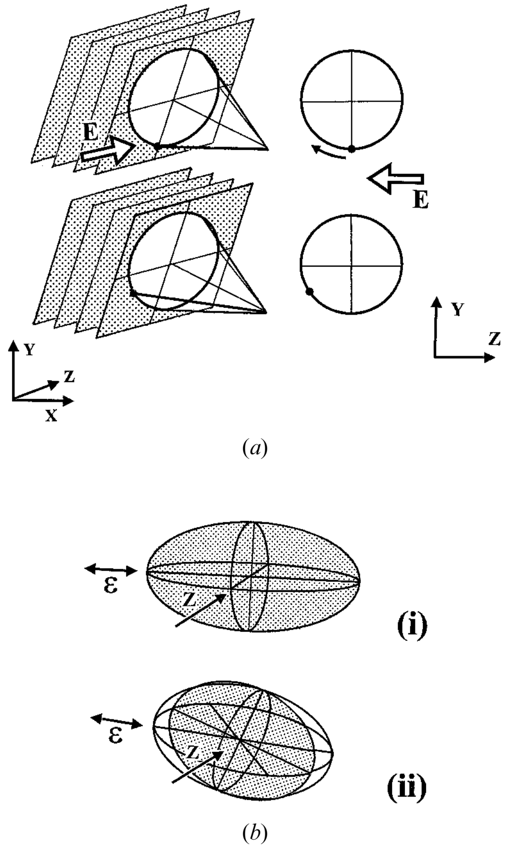

(*a*)

(*b*)

Figure 6. (*a*) The realignment of the molecules by rotation of the molecular director around an alignment cone (whilst maintaining the smectic layer organization in the cell in a more or less undisturbed state) is considered to be the first response of the cell to the applied field. This distortion can be regarded as the smectic C equivalent of the familiar Fréedericksz effect for nematic phases. In this sketch the layer alignment corresponding to the central tilted bookshelf region is shown, but similar effects will occur in the chevron arms. (*b*) Reduction in birefringence—these two sketches show the index ellipsoids corresponding to (i) the field-off state and (ii) the low-field state, the upper and lower states in (*a*). The molecular realignment would cause a change in the optical properties of reorienting the index ellipsoid so that its major axis lies more closely parallel with the Z-direction. This would reduce the perceived birefringence when the sample is viewed down the Z-direction, as indicated by the more circular shape of the shaded cross-section shown for (ii). This would lower the order of the interference colours (giving the near primary 1st order blues and yellows).

the X-ray diffraction evidence of figure 4. The data show only a small change in intensity at low fields, becoming more marked as the field increases above ~5 V μm^{-1}. This increase in scattering intensity is consistent with a higher proportion of layers moving into the Bragg condition at the rocking angle of 17° as the field increases, though admittedly the variation in intensity is not large.

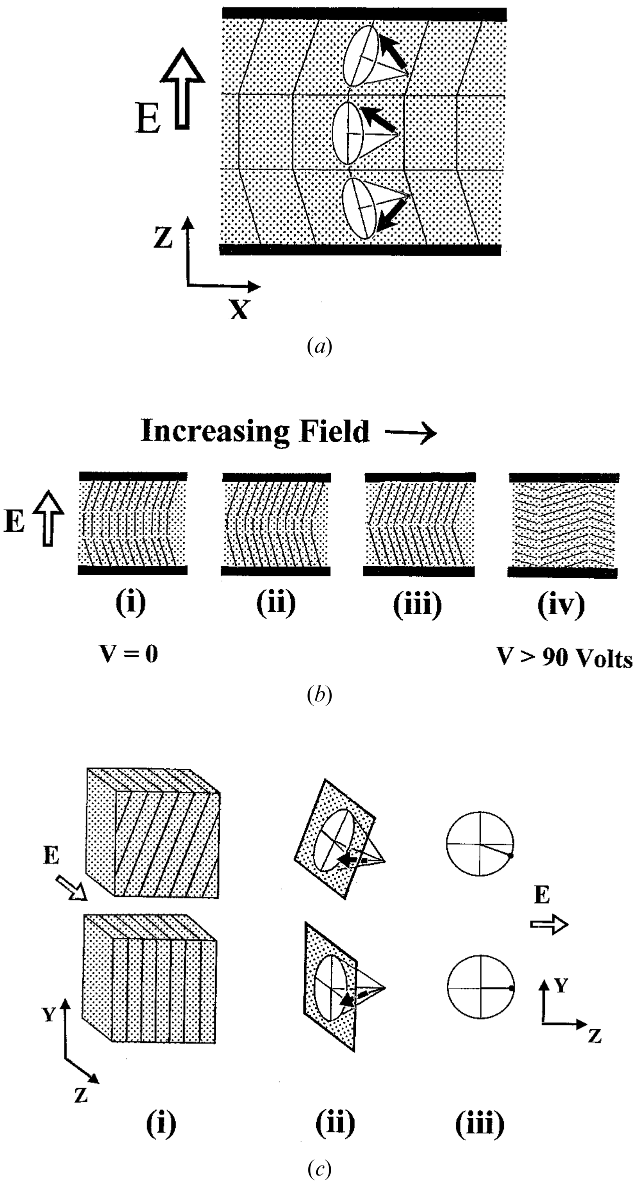

(*a*)

(*b*)

(*c*)

Figure 7. Growth of the outer chevron arms—molecules in the outer chevron arms are able to take up alignments more closely parallel to the applied field than those in the central bookshelf regions shown in (*a*). They therefore represent a lower energy state and we therefore suggest that the chevron arms grow at the expense of the central region as the field is increased. (*b*) Tilting of the layers in the XY-plane—comparison of the alignment cones for a tilted layer structure (shown in the upper sketches) and an untilted layer structure (shown in the lower sketches). It can be seen that the lower the tilt angle in the XY-plane (i.e. the more closely the layers lie parallel to the Y-axis), the more closely the molecules can align themselves along the applied field. Hence as the field is increased we would expect the tilt to be progressively reduced.

A similar consideration applies to the tilting of the layers in the XY-plane. As sketched in figure 7 (*c*) the smaller the tilt angle (i.e. the closer the layer normals

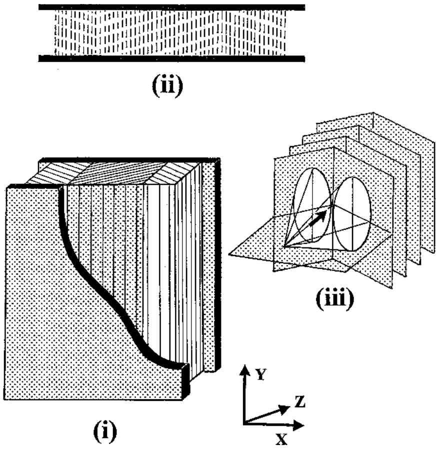

Figure 8. The final high field state. As shown in figure 2(F), the high field state (where $V > 90\ \mathrm{V_{rms}}$) consists of an array of small domains elongated along the Y-axis. There appear to be domains of only two colours, presumably indicating that there are only two orientations of these domains. The grey shades (in contrast to the bright, near-primary colours of the low field textures) suggest very low birefringence values, implying that the molecules are close to homeotropic in their alignment. We suggest that the elongation of the domains is a consequence of the bulk dimension change of the mesophase caused by the molecular realignment. As the imposed field causes the molecules to realign along Z, the structure shrinks along the X-direction. It is constrained in the Z-direction and hence attempts to expand along Y. (i) Perspective sketch view of the cell showing the elongation of the domains along Y. (ii) The inferred layer arrangement as seen in the XZ-plane, showing the two equivalent orientations of the SmC layers for a homeotropic alignment of molecular directors. (iii) Sketch showing the alignment cones at the boundary between the domain units.

lie to the X-axis) the closer the molecules can align themselves with the imposed field (in the Z-direction). We suggest that it is the combination of these two factors which explains the texture changes apparent in figure 2(B–E). If we are correct in this suggestion then the removal of the central region produces a cell with a structure similar to a SmC* chevron. Perhaps this is why the familiar defect pattern of zigzags and thick lines becomes more apparent at moderate field strengths.

During the final abrupt change, molecules are torn out of the constraints of the initial chevron pattern and realigned to give a near-homeotropic structure. Note that for a tilted layer structure of the SmC phase there are two symmetry-equivalent layer arrangements, both equally viable, for a parallel array of molecules as shown in figure 8, hence one would expect that the final state would consist of equal numbers of these. We suggest that this explains the division of the final texture into what appear to be two equally-prevalent domain types. We suggest that the elongation of the domains is a consequence of the bulk dimension change of the mesophase caused by the molecular realignment. As the imposed field causes the molecules to realign along Z, the structure shrinks along the X-direction. It is constrained in the Z-direction and hence attempts to expand along Y.

5. Conclusions

A previous paper reported the unusual three-armed chevron structure that was adopted by an achiral smectic C material in a thin, homogeneously aligned device. The electric field deformation of this complex layer geometry has been explained in terms of a four-step process, taking advantage of information gleaned from textural observations, electro-optic experiments and field-dependent X-ray scattering studies. Two distinct field-induced transitions are reported: one associated with reorientation of the *c*-director and the other with gross reorganization of the smectic layers. An interpretation of the origin of the observed phenomena in terms of director and layer motion is vital if the elastic constants of such systems are to be deduced from Fréedericksz transition experiments. A detailed study of the Fréedericksz thresholds for this system is to be reported in a future publication.

A.F. is grateful for financial support from the Displays Group, DERA, Malvern, UK. Thanks are also due to Y. Panarin for the sample of M3 and to the staff of Daresbury Laboratory for their assistance.

References

[1] J. W. Goodby, R. Blinc, N. A. Clark, S. T. Lagerwall, M. A. Osipov, S. A. Pikin, T. Sakurai, K. Yoshino, and B. Zeks (editors), 1991, Ferroelectrical Liquid Crystals. Principles, Properties and Applications, Vol. 7 of Ferroelectricity and Related Phenomena (Reading: Gordon and Breach).
[2] Matkin, L. S., Gleeson, H. F., Watson, S. J., Baylis, L., Bowring, N., Goodby, J. W., Hird, M., and Seed, A., 2000, *Appl. Phys. Lett.*, **77,** 340.
[3] Morse, A., and Gleeson, H. F., 1997, *Liq. Cryst.*, **23,** 531.
[4] Findon, A., Gleeson, H. F., and Lydon, J., 1998, *Liq. Cryst.*, **25,** 631.
[5] Carlsson, T., Stewart, I. W., and Leslie, F. M., 1992, *Liq. Cryst.*, **11,** 49.
[6] Findon, A., 1995, PhD thesis, Manchester University, UK.